CRITICAL BEHAVIOR IN NUCLEAR MULTIFRAGMENTATION*

Janusz Brzychczyk

M. Smoluchowski Institute of Physics, Jagellonian University
Reymonta 4, 30-059 Kraków, Poland

(Received April 10, 2000)

Fluctuations of the fragment-size distribution have been studied in the framework of a bond percolation model using the method of scaled factorial moments (SFM). The independence of SFM from fragment-size resolution but not power-law behavior (intermittency) characterizes the fluctuations at the percolation transition. The SFM determined for various individual fragment-size intervals converge to a value of ~ 1 near the critical point. The convergence occurs even in very small systems, and events may be sorted according to measurable quantities. This may serve as a new possible signature of critical behavior in nuclear multifragmentation.

PACS numbers: 24.60.Ky, 25.70.Pq

In recent years the occurrence of critical behavior in nuclear multifragmentation has been the subject of intensive study inspired by the prediction of liquid–gas phase transition in nuclear matter [1–3], the observation fragment mass distributions exhibiting a power-law dependence [4], and by the resemblance between nuclear multifragmentation data and predictions of percolation models which are known to contain critical behavior [5–7]. Various methods have been proposed to reveal the trace of critical behavior in fragmenting systems. In particular, Ploszajczak and Tucholski suggested a search for intermittency in fluctuations of the fragment-size distribution [8]. Intermittency corresponds to self-similar fluctuations on all scales and can be deduced from the power-law behavior of SFM [9]. Intermittent-like signals have been found in percolation models [8], classical molecular dynamics simulations [10–12], and statistical models [13–15], as well as in some nuclear

* Presented at the Kazimierz Grotowski 70$^{\rm th}$ Birthday Symposium "Phases of Nuclear Matter", Kraków, Poland, January 27–28, 2000.

multifragmentation data [8,16–18]. However, the interpretation of these signals as a manifestation of critical behavior is doubtful. The properties of the anomalous fractal dimensions are inconsistent with those predicted for second-order phase transitions [8,13,14,17]. On the other hand, such signals may appear, even in the absence of a critical phenomenon, due to finite-size effects, the mixing of different types of events, and/or the specific shape of the mean fragment-size distribution [15, 19–24]. The criticality origin of the signals is not confirmed even for percolation models. A signal suggestive of intermittency, observed for small lattices close to the critical point, disappears when the size of the system goes to infinity. Moreover, an analysis made for near-critical events at fixed multiplicity or within some range of multiplicities shows no evidence of intermittency [22, 24]. Campi and Krivine concluded that the signal has been incorrectly interpreted as a genuine intermittency [22].

If the intermittency concept is irrelevant to fragment-size fluctuations, it is natural to ask whether any other feature of these fluctuations can be identified as a sign of critical behavior. We aim to address this question in the present work. On the first attempt we examine percolation processes.

The intermittency analysis performed in earlier works employs horizontally averaged SFM, $\bar{F}_i$, defined as [8, 25]

$$\bar{F}_i(\delta s) = \frac{\sum_{j=1}^{M} \langle n_j(n_j-1)\dots(n_j-i+1)\rangle}{\sum_{j=1}^{M}\langle n_j\rangle^i}. \tag{1}$$

Here, the fragment-size axis is divided into M bins of equal size $\delta s = S_0/M$, where S_0 denotes the system size, n_j is the number of fragments in the j-th bin for a given event, and the brackets indicate averaging over the set of events under consideration. Intermittency is deduced when the factorial moments $\bar{F}_i$ increase like a power-law with decreasing δs. As was already pointed out [14, 22, 26], the disadvantage of definition (1) is that the $\bar{F}_i$ are dominated by the contributions from the first bins containing the lightest fragments. In order to inspect the whole range of fragment sizes with no constraints we study SFM for individual fragment-size intervals, $[s_a, s_b]$,

$$F_i(s_a, s_b) = \frac{\langle n(n-1)\dots(n-i+1)\rangle}{\langle n\rangle^i}, \tag{2}$$

where $n = n(s_a, s_b)$ is the number of fragments of size $s_a \le s \le s_b$ produced in an event. All possible intervals $1 \le s_a \le s_b \le S_0$ are considered. The calculations have been performed with the three-dimensional bond percolation model on simple cubic lattices. Events have been generated for randomly distributed values of the bond-breaking probability, p, and then grouped in bins of the following variables: the probability p, the fraction of broken bonds, k, the normalized overall multiplicity, $m = n(1, S_0)/S_0$, and the normalized total size of complex fragments, $z = S_{\text{bound}}/S_0 = 1 - n(1,1)/S_0$. Below we will show the results of the calculations for the $6 \times 6 \times 6$ lattice, which are representative of small systems.

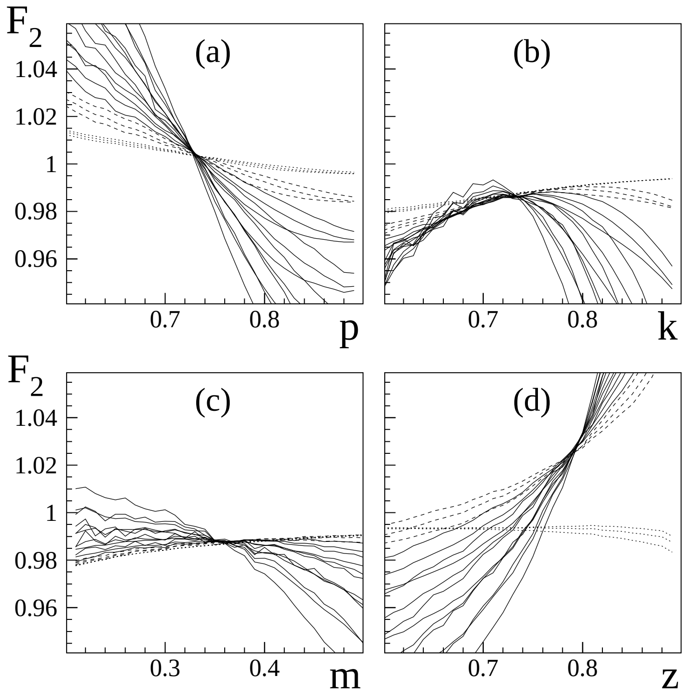

Fig. 1. Predictions of the bond percolation model with 6^3 sites. The second-order scaled factorial moment, F_2, as a function of: (a) the bond-breaking probability, (b) the fraction of broken bonds, (c) the normalized total multiplicity, (d) the normalized total size of complex fragments. Lines represent $F_2(s_a, s_b)$ calculated for 18 various fragment-size intervals $[s_a, s_b]$, where $s_a = 1$ (dotted), 2 (dashed), 3, 4, 5, 6 (solid), and $s_b = (s_a + 3)$, $(s_a + 7)$, 20.

Fig. 1 displays $F_2(s_a, s_b)$ plotted as a function of p, k, m, and z for various fragment-size intervals. The lines shown in these plots represent $s_a = 1, 2, \ldots 6$ with $s_b = (s_a+3)$, (s_a+7), 20. The dotted, dashed, and solid lines are for $s_a = 1$, $s_a = 2$, and $s_a > 2$, respectively. Generally, the lines are steeper for larger clusters, *i.e.* for larger s_a and/or s_b. Statistical errors in these simulations are reflected in the line oscillations. Here, 8×10^6 events have been generated in the range $0.45 < p < 0.95$. The most prominent feature of these results, observed for all the binnings, is the convergence of $F_2(s_a, s_b)$ values corresponding to different fragment-size intervals $[s_a, s_b]$.

The exception seen in Fig. 1(d) for $s_a = 1$ (dotted lines) is understandable. The quantity z is defined by $n(1, 1)$, dominant in $n(1, s_b)$. As a result, the fluctuations of $n(1, s_b)$ are strongly suppressed when z is fixed. The value of F_2 at the convergence point may be slightly greater or less than 1 depending on the choice of binning variable. In the case of the control parameter, p, the lines intersect at $p \simeq 0.73$, which is close to the critical point in the continuos limit, $p_c = 0.7512$ [7]. This suggests that the convergence effect is associated with the percolation phase transition. The positions of the crossing points for other binnings correspond to that for p: events with $p = 0.73$ are characterized by $\langle k\rangle = 0.73$, $\langle m\rangle \simeq 0.344$, and $\langle z\rangle \simeq 0.787$.

Regardless of some possible exceptions, such as that for binning by z when $s_a = 1$, the convergence of $F_2(s_a, s_b)$ occurs for all fragment-size intervals $[s_a, s_b]$ as long as s_b is relatively small in comparison to the system size, S_0. For example, Fig. 2(a) shows $F_2(s_a, s_b)$ *versus* p for $s_a = 3$ and s_b ranging from 4 to $S_0 = 216$. The lines are well focused if $s_b <\sim 30$ (solid lines). The departures of the lines with $s_b > 30$ from the convergence point seem to be related to the fluctuations of the size of the largest fragment produced per event, $s_{\max}$. Fig. 2(b) presents the event-by-event correspondence between $s_{\max}$ and the control parameter. One may observe that around $p = 0.73$ fragment-size intervals with $s_b > 30$ overlap the region covered by $s_{\max}$. This correlation is confirmed by calculations performed on different lattices. An approximate limit for the presence of the convergence in small systems can be given as $s_b < 2\sqrt{S_0}$.

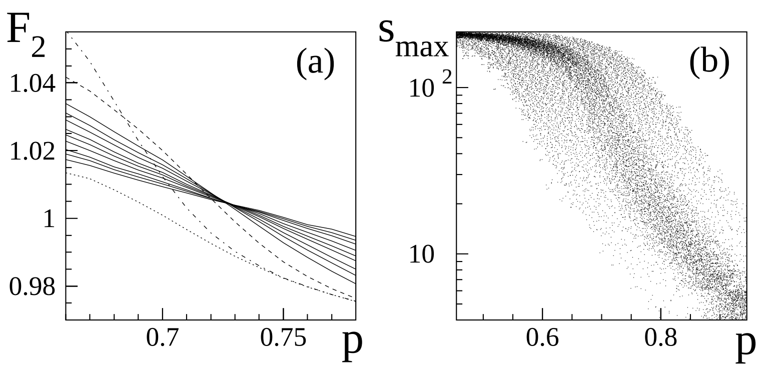

Fig. 2. Bond percolation model with 6^3 sites. Plotted as a function of p: (a) $F_2(s_a, s_b)$ for $s_a = 3$ and $s_b = 4$, 5, 6, 8, 10, 12, 16, 20, 27 (solid), 54 (dashed), 108 (dot-dashed), 216 (dotted). (b) the size of the largest cluster produced per event, $s_{\max}$.

Besides F_2 we have also examined the higher-rank factorial moments F_3 and F_4. They reflect the behavior of F_2 according to the following approximate scaling

$$(F_3 - 1) \simeq 3(F_2 - 1), \qquad (F_4 - 1) \simeq 6(F_2 - 1), \tag{3}$$

This scaling is particularly accurate in the critical regime. Given $|F_2 - 1| \ll 1$ and the relations between the scaled factorial moments, F_i, and the scaled factorial cumulants, K_i, [27]

$$\begin{aligned} F_2 &= 1 + K_2\,, \\ F_3 &= 1 + 3K_2 + K_3\,, \\ F_4 &= 1 + 6K_2 + 4K_3 + 6K_2^2 + K_4\,, \end{aligned} \tag{4}$$

the presence of the scaling (3) indicates that F_i are determined by K_2, *i.e.* contributions from the higher-order cumulants are negligible. It should be noted that this dominance of two-particle correlations in SFM has been already found in percolation by Lacroix and Peschanski [26].

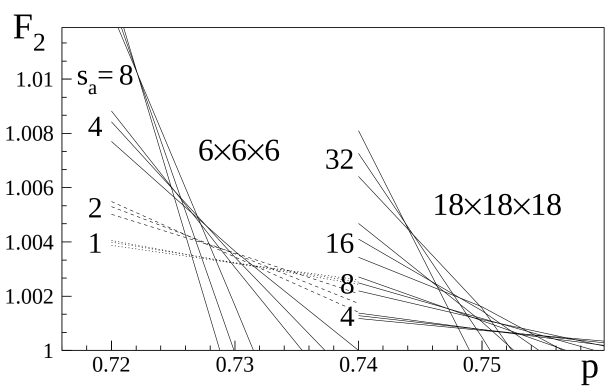

Fig. 3. $F_2(s_a, s_a + \delta s - 1)$ *versus* p for the 6^3 and 18^3 percolation systems. s_a values are indicated on the figure, $\delta s = 6$, 10, 14 for the smaller system, $\delta s = 32$, 64, 128 for the larger one.

In order to explore how the convergence of $F_2(s_a, s_b)$ is affected by finite-size constraints, in Fig. 3 we have compared the results for the small $6 \times 6 \times 6$ and larger $18 \times 18 \times 18$ lattices. In the case of the small system, the lines representing various $[s_a, s_b]$ intervals ($s_a = 1$, 2, 4, 8; $\delta s = s_b - s_a + 1 = 6$, 10, 14) intersect in a region located between $p = 0.72$ and 0.74. The lines with the same s_a are well focused and form a distinct bundle. The intersection points from different bundles are somewhat dispersed, but this effect may be not even noticeable in practical tests, such as that in Fig. 1.

For the larger system, avoiding $s_{\max}$ by applying the condition $s_b < 150$, we have plotted lines for $s_a = 4, 8, 16, 32$ with $\delta s = 32, 64, 128$. Here, the crossing points are much closer to the critical point. This fact corroborates connection between the convergence effect and the percolation transition. Departures of the convergence points from $p = p_c$ and $F_2 = 1$ can be seen as a finite-size effect. It is noteworthy that the convergence is clearly observed even in systems with as few as 64 constituents. For the $4 \times 4 \times 4$ lattice and $s_b < 15$, the crossings are observed at $p \simeq 0.70$, $k \simeq 0.72$, $m \simeq 0.39$, $z \simeq 0.80$, and $F_2 \simeq 1.015, 0.97, 0.97, 1.09$, respectively.

At the convergence point SFM are independent of the fragment-size resolution. We believe that this feature, which contradicts the presence of intermittency, is attributed to the critical behavior. However, intermittent-like signals may be found near the convergence point, and thus in the vicinity of the critical point. For example, Ploszajczak and Tucholski found such signals in the bond percolation model containing 6^3 sites within a narrow range of bond parameters q, equivalent to $0.73 \leq p < 0.79$ [8]. As previously mentioned, the horizontally averaged SFM, $\bar{F}_i$, used in that analysis can be well approximated by F_i calculated for the first bins: $\bar{F}_i(\delta s) \simeq F_i(s_a = 1, \delta s)$. The solid lines in Fig. 4(a) display $F_2(s_a = 1, \delta s)$ for $\delta s = 1, 2, 4, 8, 14$ (the larger the δs the steeper the line). It is clear that $F_2(p = \text{const.}, \delta s)$ increases with decreasing δs when $p > 0.73$. In this "overcritical" region, F_2 values are less than 1 except for a narrow interval of p close to the convergence point. This exception is possible only in finite systems. The plot $\ln(F_i)$ *versus* $-\ln(\delta s)$ shown in Fig. 4(b) corresponds to $p = 0.77$, called in Ref. [8] the "optimal" value. F_3 and F_4 follow F_2 according to the scaling (3). The points connected by the solid lines are for $F_i(s_a = 1) \simeq \bar{F}_i$. As can be deduced from Fig. 4(a), this is the case when, with the requirement $F_i(s_a = 1) > 1$ for $\delta s < 15$, the slopes are maximal. The linear rise observed in this plot was interpreted as a signal of intermittency. However, such a "signal" appears here only for the first bins containing the lightest fragments. It vanishes when the lightest fragments are excluded from the analysis: the dashed lines in Fig. 4 show the results for $s_a = 2$. In contrast to the convergence effect, the intermittent-like signal is limited to the specific event selection. In particular, Fig. 1(c) shows that $F_i < 1$ when selecting events with the same multiplicity. This example illustrates how the observations made by the authors of Ref. [8], and also by Campi and Krivine [22], can be understood in the context of our results.

It is worth noting that the multiplicity distributions in $[s_a, s_b]$ intervals at the convergence point cannot be described by a certain type of standard distributions (binomial, Poissonian, Gaussian, *etc.*). Their coefficients, such as the skewness, the sharpness, and the ratio of variance to mean, vary with the choice of s_a, s_b and binning variable. The latter coefficient may be

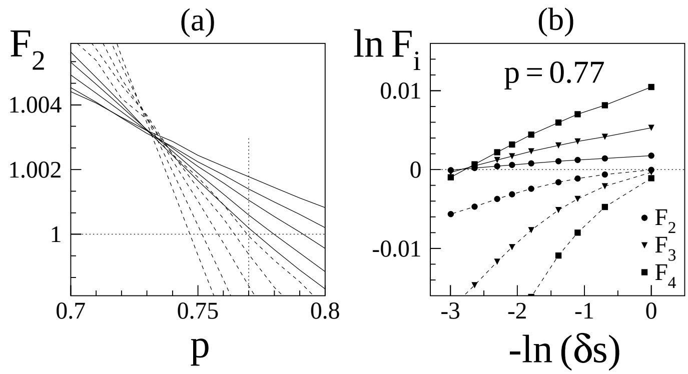

Fig. 4. SFM in the bond percolation model with 6^3 sites for $s_a = 1$ (solid lines) and $s_a = 2$ (dashed lines): (a) $F_2(\delta s)$ *versus* p for $\delta s = 1, 2, 4, 8, 14$, (b) the dependence of F_2, F_3, and F_4 on the width of the fragment-size interval, δs, for events with $p = 0.77$.

greater or less than 1, *i.e.* both sub- and super-Poissonian distributions are observed. The properties of such coefficients have been discussed recently in Refs. [26, 28]. We have not found any feature of these parameters to be as distinct as the convergence of SFM, which could serve as an alternative signature of critical behavior.

In conclusion, a bond percolation model has been used to study event-to-event fluctuations of the fragment-size distribution in small systems. We have examined the properties of SFM of the multiplicity distributions in individual fragment-size intervals $[s_a, s_b]$, using various quantities to categorize percolation events: the bond-breaking probability, the fraction of broken bonds, the total multiplicity and the total size of complex fragments. For each sorting variable, the values of $F_2(s_a, s_b)$ calculated for different intervals ($s_b \ll S_0$) converge to a value close to 1 near the critical condition. The higher-order SFM are related to F_2 according to the dominance of the second-order cumulant. Calculations performed for a larger system confirm that the convergence effect is closely connected with the percolation transition.

It will be interesting to verify the presence of the convergence in nuclear multifragmentation. This new possible signature of critical behavior shows some valuable features. It may be observed in very small systems, and events may be sorted according to different measurable quantities. In the present work we have checked the total multiplicity and the total mass/charge of complex fragments. Presumably, other binning variables can be also applied. It would be worthwhile to test some selections which are related to intermediate mass fragments to avoid uncertainties associated with light fragments due to preequilibrium emission and secondary evaporation. Accordingly, the convergence could be examined for fragment-size intervals which do not include light particles.

It remains an open question whether the convergence effect for SFM is characteristic of the percolation transition only, or is a more general feature of critical behavior. It will be instructive to perform the analysis for models containing different types of critical behavior, *e.g.* second-order phase transitions from other universality classes.

The SFM method is a valuable tool for studying fluctuations in fragment-size distributions. However, with respect to using averaged SFM, better insight can be obtained into the properties of the fluctuations when the set of SFM values corresponding to all individual fragment-size intervals is examined.

REFERENCES

[1] P.J. Siemens, *Nature* **305**, 410 (1983).

[2] H. Jaqaman, A.Z. Mekjian, L. Zamick, *Phys. Rev.* **C27**, 2782 (1983); **C29**, 2067 (1984).

[3] A.L. Goodman, J.I. Kapusta, A.Z. Mekjian, *Phys. Rev.* **C30**, 851 (1984).

[4] J.E. Finn *et al.*, *Phys. Rev. Lett.* **49**, 1321 (1982).

[5] W. Bauer *et al.*, *Nucl. Phys.* **A452**, 699 (1986); W. Bauer *et al.*, *Phys. Rev. Lett.* **58**, 863 (1987); W. Bauer, A. Botvina, *Phys. Rev.* **C52**, R1760 (1995).

[6] X. Campi, *J. Phys.* **A19**, L917 (1986); *Phys. Lett.* **B208**, 351 (1988).

[7] D. Stauffer, A. Aharony, *Introduction to percolation theory*, 2nd Edition, Taylor & Francis, London 1992.

[8] M. Ploszajczak, A. Tucholski, *Phys. Rev. Lett.* **65**, 1539 (1990); *Nucl. Phys.* **A523**, 651 (1991).

[9] A. Bialas, R. Peschanski, *Nucl. Phys.* **B273**, 703 (1986); *Nucl. Phys.* **B308**, 857 (1988).

[10] V. Latora, M. Belkacem, A. Bonasera, *Phys. Rev. Lett.* **73**, 1765 (1994).

[11] M. Belkacem *et al.*, *Phys. Rev.* **C54**, 2435 (1996).

[12] V.N. Kondratyev, H.O. Lutz, S. Ayik, *J. Chem. Phys.* **106**, 7766 (1997).

[13] D.H.E. Gross, A.R. DeAngelis, H.R. Jaqaman, Pan Jicai, R. Heck, *Phys. Rev. Lett.* **68**, 146 (1992).

[14] A.R. DeAngelis, D.H.E. Gross, R. Heck, *Nucl. Phys.* **A537**, 606 (1992).

[15] W.A. Friedman, *Phys. Rev.* **C46**, R1595 (1992).

[16] P.L. Jain, G. Singh, M.S. El-Nagdy, *Phys. Rev. Lett.* **68**, 1656 (1992).

[17] M. L. Cherry *et al.*, *Phys. Rev.* **C53**, 1532 (1996).

[18] P. F. Mastinu *et al.*, *Phys. Rev. Lett.* **76**, 2646 (1996).

[19] H.W. Barz, J.P. Bondorf, R. Donangelo, I.N. Mishustin, H. Schulz, K. Sneppen, *Phys. Rev.* **C45**, R2541 (1992).

[20] B. Elattari, J. Richert, P. Wagner, *Nucl. Phys.* **A560**, 603 (1993).

[21] P. Desesquelles, A.J. Cole, Report No. IN2P3-CNRS, ISN 93.87, 1993; A.J. Cole, P. Desesquelles, *Phys. Rev.* **C50**, 329 (1994).

[22] X. Campi, H. Krivine, *Nucl. Phys.* **A589**, 505 (1995).

[23] L. Phair, Th. Rubehn, L.G. Moretto, G.J. Wozniak, *Phys. Rev. Lett.* **79**, 3538 (1997).

[24] Yu. Murin, R. Ghetti, B. Jakobsson, *Phys. Rev.* **C55**, 528 (1997).

[25] K. Fialkowski, B. Wosiek, J. Wosiek, *Acta Phys. Pol.* **B20**, 639 (1989).

[26] D. Lacroix, R. Peschanski, *Nucl. Phys.* **A615**, 207 (1997).

[27] P. Carruthers, H.C. Eggers, I. Sarcevic, *Phys. Lett.* **B254**, 258 (1991).

[28] T. Gharib, W. Bauer, S. Pratt, *Phys. Lett.* **B444**, 231 (1998).